

Data-Efficient Error Mitigation for Physical and Algorithmic Errors in a Hamiltonian Simulation

Shigeo Hakkaku,^{1, 2, *} Yasunari Suzuki,^{1, 2} Yuuki Tokunaga,^{1, 2} and Suguru Endo^{1, 2, 3, †}

¹*NTT Computer and Data Science Laboratories, NTT, Inc., 3-9-11 Midori-cho, Musashino, Tokyo 180-8585, Japan*

²*NTT Research Center for Theoretical Quantum Physics, NTT, Inc., 3-1 Morinosato-Wakamiya, Atsugi 243-0198, Japan*

³*JST, PRESTO, 4-1-8 Honcho, Kawaguchi, Saitama, 332-0012, Japan*

Quantum dynamics simulation via Hamiltonian simulation algorithms is one of the most crucial applications in the quantum computing field. While this task has been relatively considered the target in the fault-tolerance era, the experiment for demonstrating utility by an IBM team simulates the dynamics of an Ising-type quantum system with the Trotter-based Hamiltonian simulation algorithm with the help of quantum error mitigation [1]. In this study, we propose the data-efficient 1D extrapolation method to mitigate not only physical errors but also algorithmic errors of Trotterized quantum circuits in both the near-term and early fault-tolerant eras. Our proposed extrapolation method uses expectation values obtained by Trotterized circuits, where the Trotter number is selected to minimize both physical and algorithmic errors according to the circuit's physical error rate. We also propose a method that combines the data-efficient 1D extrapolation with purification QEM methods, which improves accuracy more at the expense of multiple copies of quantum states or the depth of the quantum circuit. Using the 1D transverse-field Ising model, we numerically demonstrate our proposed methods and confirm that our proposed extrapolation method suppresses both statistical and systematic errors more than the previous extrapolation method.

I. INTRODUCTION

One of the most promising applications of a fault-tolerant quantum computer is simulating dynamics of many-body problems, such as condensed matter physics and quantum chemistry [2, 3]. Hamiltonian simulation algorithms have been mainly discussed in the regime of fault tolerance, and numerous improvements have been made in this area [4–10]. Although most such algorithms are beyond the capacity of the current quantum computers, the Trotter-based Hamiltonian simulation algorithm has already been performed in the current quantum device by an IBM team, with the utility of quantum devices being investigated [1].

In the above experiment, the error-extrapolation quantum error mitigation (QEM)[11–13] has played a crucial role in improving the accuracy of the simulation result by suppressing the physical errors due to coupling to the environment. Besides the near-term application, it has been pointed out that QEM can significantly improve the computation accuracy of quantum algorithms in the early fault-tolerant quantum computing (FTQC) era and contribute to reducing resources such as code distances and T gate counts [14–18].

While the primary target of QEM has been the suppression of physical errors, the computation accuracy of quantum algorithms is also restricted by algorithmic errors because of the insufficiency of the circuit depth. Ref. [19] elaborated a QEM method tailored to noisy

Trotterized quantum circuits to suppress both the algorithmic and physical errors. This method uses error-extrapolation QEM methods to mitigate physical error rates and then applies the algorithmic error extrapolation method for Trotter-based quantum simulation by leveraging the outcomes for fewer Trotter steps. Although this method does not impose any additional hardware requirements and may enhance computation accuracy even in current quantum devices, the variance of its estimator is relatively large. This is because the method performs two successive extrapolations, thereby requiring many noisy expectation values.

In this work, we propose a data-efficient error extrapolation method for physical and algorithmic errors, which is an even more robust QEM for Trotter-based quantum algorithms. The proposed extrapolation method uses expectation values obtained by Trotterized circuits where the Trotter number is selected to minimize both physical and algorithmic errors as a function of the physical error rate of the circuit. Our proposed method performs only one extrapolation according to the physical noise, and it gives a more accurate result than sequentially applying extrapolation for physical and algorithmic errors. To identify such a Trotter number, we clarify the dependence of the optimal Trotter numbers on the error rates of physical noise by evaluating the distance between the exact time-evolved operator and the noisy Trotterized circuit. Then, by analyzing an output state of the noisy Trotterized circuit with such a Trotter number, we discuss the coefficients of the proposed extrapolation method.

We also propose a method that combines the proposed data-efficient error extrapolation with purification QEM methods [20–23], which improves accuracy even more at the expense of the number of copies of quantum states or

* shigeo.hakkaku@ntt.com

† suguru.endou@ntt.com

the depth of the quantum circuit. We dub this method as Trotter subspace expansion. The Trotter subspace expansion ensures that the error-mitigated computation outcome leads to the physical one. We construct the error-mitigated state $\rho_{\text{QEM}} = \frac{\rho_{\text{extra}}^2}{\text{Tr}[\rho_{\text{extra}}^2]}$ for the effective state of the proposed extrapolation method $\rho_{\text{extra}} = \sum_i c_i \rho(p_i)$ ($c_i \in \mathbb{R}$) by the help of the purification-based QEM methods. Here, $\rho(p_i)$ are noisy output states with p_i being the different physical error rates, where the Trotter number is chosen to minimize the physical and algorithmic errors.

To benchmark our proposed methods, we numerically compare them with the existing error mitigation method proposed in Ref. [19] under finite measurements by considering the dynamics of 1D transverse field Ising model with 10 qubits. We find that the MSE of the data-efficient extrapolation is the least in some existing QEM methods if $10^8 \leq N \leq 10^{11}$. Also, the numerical result shows that the Trotter subspace expansion would be more useful than the data-efficient extrapolation if we could use at least 10^{12} number of measurements. Its converged MSE is 710 times smaller than the raw data and 31 times smaller than the data-efficient extrapolation. Thus, if we can execute many quantum computers in parallel, the Trotter subspace expansion would be more useful than the other QEM methods.

II. PRELIMINARIES

In this section, we review the error extrapolation method for Trotter errors [19]. Then, we explain purification-based quantum error mitigation methods, which use multiple copies of noisy quantum states. We combine these methods with our proposed extrapolation method, as we will see later in Sec. III.

A. Trotterization

Here, we give a brief explanation of the Trotterization [4, 5]. The Trotterization approximates an exponential of a sum of operators, such as a time evolution operator, by a product of elementary exponentials. Thus, it is used as a subroutine of many quantum algorithms, including Gibbs state preparation [24], Hamiltonian simulation [4], and phase estimation [25, 26]. In the following, we explain the Trotterization using a time evolution operator as an example. Let $H = \sum_j H_j$, where each H_j acts on a constant number of qubits. The time evolution operator e^{-iHt} can be approximated by a product of unitaries e^{-it/MH_j} :

$$\exp(-iHt) = \left[\prod_j \exp\left(-i\frac{t}{M} H_j\right) \right]^M + \mathcal{O}\left(\frac{t^2}{M}\right),$$

where M is called the Trotter number or Trotter step and $\mathcal{O}\left(\frac{t^2}{M}\right)$ is an algorithmic error. Therefore, M determines the level of algorithmic error. If quantum circuits are error-free, the algorithmic error can be arbitrarily suppressed as the Trotter number increases. Denoting $\epsilon_M = 1/M$ and U_{ϵ_M} as

$$U_{\epsilon_M}(t) := \left[\prod_j \exp(-i\epsilon_M t H_j) \right]^{1/\epsilon_M},$$

we can obtain

$$\lim_{\epsilon_M \rightarrow +0} U_{\epsilon_M}(t) = \exp(-iHt). \quad (1)$$

However, we cannot increase M infinitely because current quantum devices suffer from noise. In such a device, a number of Trotter steps introduces more physical errors, and thus, there exists the optimal Trotter number M_{opt} [27]. Denoting the ideal and noisy quantum process of one layer of the Trotterization, i.e., $\prod_j \exp(-i\frac{t}{M} H_j)$ as \mathcal{U}_{TR} and \mathcal{E}_{TR} , respectively, the distance between the target process $\mathcal{U}_{\text{targ}} := [e^{-iHt}]$, where $[A](\sigma) = A\sigma A^\dagger$, and the noisy Trotterized process reads:

$$\begin{aligned} D(\mathcal{U}_{\text{targ}}, \mathcal{E}_{\text{TR}}^M) &\leq M D(\mathcal{U}_{\text{targ}}^{\frac{1}{M}}, \mathcal{E}_{\text{TR}}) \\ &\leq M \left\{ D\left(\mathcal{U}_{\text{targ}}^{\frac{1}{M}}, \mathcal{U}_{\text{TR}}\right) + D(\mathcal{E}_{\text{TR}}, \mathcal{U}_{\text{TR}}) \right\}. \end{aligned} \quad (2)$$

Here, $D(\mathcal{E}_1, \mathcal{E}_2) = \max_{\sigma} \|\mathcal{E}_1(\sigma) - \mathcal{E}_2(\sigma)\|_1$ is the distance between two quantum processes \mathcal{E}_1 and \mathcal{E}_2 for the trace norm $\|A\| = \text{Tr}[\sqrt{A^\dagger A}]$ with σ being the properly chosen quantum states [28]. Note that we assume the noise process for each layer is the same. In the first line of Eq. (2), we use the chaining property $D(\mathcal{E}_1 \circ \mathcal{E}'_1, \mathcal{E}_2 \circ \mathcal{E}'_2) \leq D(\mathcal{E}_1, \mathcal{E}'_1) + D(\mathcal{E}_2, \mathcal{E}'_2)$. In the second line, we use the triangle inequality. Since we have $D(\mathcal{U}_{\text{targ}}^{\frac{1}{M}}, \mathcal{U}_{\text{TR}}) \leq \frac{a}{M^2}$ and $D(\mathcal{E}_{\text{TR}}, \mathcal{U}_{\text{TR}}) \leq b$ for some constants $a, b > 0$, we get:

$$D(\mathcal{U}_{\text{targ}}, \mathcal{E}_{\text{TR}}^M) \leq \frac{a}{M} + bM,$$

which indicates that there is an optimized Trotter number $M_{\text{opt}} = \sqrt{\frac{a}{b}}$. See Refs. [19, 27] for details.

B. Trotter Error Extrapolation

In this section, we review how to suppress the algorithmic error introduced in Sec. II A according to Ref. [19]. This method suppresses the algorithmic error by regarding an inverse of the Trotter number as an “error rate” in the standard polynomial error extrapolation method.

Suppose that one applies the unitary operator $U_{\epsilon_M}(t)$ to the state $|\psi\rangle$, then the expectation value of an observable A is given by

$$\langle A(t) \rangle (\epsilon_M) = \langle \psi | U_{\epsilon_M}^\dagger(t) A U_{\epsilon_M}(t) | \psi \rangle.$$

Expanding $\langle A(t) \rangle (\epsilon_M)$ as a function of ϵ_M gives

$$\langle A(t) \rangle (\epsilon_M) = \langle A(t) \rangle (0) + \sum_{i=1}^{n'} A(t)_i \epsilon_M^i + \mathcal{O}(\epsilon_M^{n'+1}), \quad (3)$$

where $\langle A(t) \rangle (0) = \langle \psi | \exp(iHt) A \exp(-iHt) | \psi \rangle$ i.e., the algorithmic-error-free expectation value of A , and $\langle A(t)_i \rangle$ stand for the real coefficients of the expansion.

From Eqs. (1) and (3), we can confirm that the error extrapolation method can be applied with algorithmic errors by reducing the Trotter number. Normally, we increase the Trotter step up to M_{opt} . Combining the set of data points with different Trotter steps $\{\langle A(t) \rangle (\epsilon_{M_i})\}_{i=0}^{n'}$, where $M_{n'} \leq \dots \leq M_1 \leq M_0 = M_{\text{opt}}$, with Eq. (3), we obtain

$$\begin{aligned} \langle A \rangle_{\text{est}}(0) &= \sum_{i=0}^{n'} \langle A \rangle (\epsilon_{M_i}) \prod_{k \neq i} \frac{\epsilon_{M_k}}{\epsilon_{M_k} - \epsilon_{M_i}} \\ &= \langle A \rangle (0) + \mathcal{O}(\epsilon_{M_{\text{opt}}}^{n'+1}). \end{aligned}$$

Thus, we see that the algorithmic error can be suppressed to $\mathcal{O}(\epsilon_{M_{\text{opt}}}^{n'+1}) = \mathcal{O}(M_{n'}^{-(n'+1)})$.

The variance of the estimator $\langle A \rangle_{\text{est}}(0)$ is given by

$$\text{Var}[A_{\text{est}}(0)] = \sum_{i=0}^{n'} \text{Var}[A(\epsilon_{M_i})] \left(\prod_{k \neq i} \frac{\epsilon_{M_k}}{\epsilon_{M_k} - \epsilon_{M_i}} \right)^2.$$

Then, the required sampling cost of the estimator within the additive error δ is given by $\mathcal{O}(\delta^{-2} \text{Var}[A_{\text{est}}(0)])$.

III. DATA-EFFICIENT PHYSICAL AND ALGORITHMIC EXTRAPOLATION

Here, we introduce a data-efficient physical and algorithmic error extrapolation method, which suppresses statistical errors more than the previous method [19]. In this method, we select data points on a line in the plane with axes representing physical error and inverse of Trotter error. In the following, we will explain the relationship between the optimal Trotter number M_{opt} and the error rate of the global depolarizing noise p_{global} , i.e., $M_{\text{opt}} \propto 1/\sqrt{p_{\text{global}}}$, thereby providing a 1D extrapolation method.

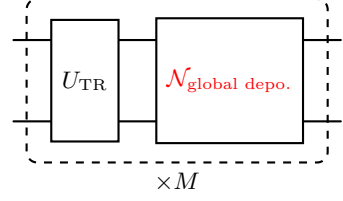


FIG. 1. Schematic circuit for deducing an optimal Trotter number as a function of the error rate of the global depolarizing noise. U_{TR} is one layer of the Trotterization, M is the Trotter number, and $\mathcal{N}_{\text{global depo.}}$ is the global depolarizing noise.

A. Optimal Trotter Number

Suppose that the global depolarizing channel $\mathcal{N}_{\text{global depo.}}$ occurs after one layer of the Trotterization of the n -qubit target process \mathcal{U}_{TR} as shown in Fig. 1. The global depolarizing noise is defined as

$$\mathcal{N}_{\text{global depo.}}(\rho) = (1 - p_{\text{global}})\rho + \frac{p_{\text{global}}}{2^n} I^{\otimes n}.$$

Although we use the global depolarizing channel for simplicity, recent studies [29, 30] show that the local noise in a quantum circuit can be approximated as the global depolarizing noise in the large-depth regime theoretically and numerically. Therefore, the relationship that we will see later is also expected to be valid in the large-depth regime.

From the chaining property, the second term on the right-hand side of Eq. (2) follows that

$$\begin{aligned} D(\mathcal{E}_{\text{TR}}, \mathcal{U}_{\text{TR}}) &= D(\mathcal{N}_{\text{global depo.}} \circ \mathcal{U}_{\text{TR}}, \mathcal{U}_{\text{TR}}) \\ &= D([I^{\otimes n}], \mathcal{N}_{\text{global depo.}}) \end{aligned} \quad (4)$$

Then, $D([I^{\otimes n}], \mathcal{N}_{\text{global depo.}})$ can be rewritten as

$$\begin{aligned} &D([I^{\otimes n}], \mathcal{N}_{\text{global depo.}}) \\ &= \max_{\sigma} \left\| \sigma - \left\{ (1 - p_{\text{global}})\sigma + \frac{p_{\text{global}}}{2^n} I^{\otimes n} \right\} \right\| \\ &= p_{\text{global}} \max_{\sigma} \left\| \sigma - \frac{1}{2^n} I^{\otimes n} \right\|. \end{aligned} \quad (5)$$

Substituting Eq. (5) into Eq. (4), we obtain

$$D(\mathcal{E}_{\text{TR}}, \mathcal{U}_{\text{TR}}) = p_{\text{global}} \max_{\sigma} \left\| \sigma - \frac{1}{2^n} I^{\otimes n} \right\|.$$

From the above equation, we see that the distance between \mathcal{E}_{TR} and \mathcal{U}_{TR} could be proportional to p_{global} , i.e., $D(\mathcal{E}_{\text{TR}}, \mathcal{U}_{\text{TR}}) \propto p_{\text{global}}$. Thus, an optimized Trotter number could be given by

$$M_{\text{opt}} = \text{floor} \left(\frac{c}{\sqrt{p_{\text{global}}}} \right) \quad (6)$$

for a positive constant c , which would depend on the number of qubits n , the simulation time t , and the parameters of a given Hamiltonian, as we will see later.

We expect that if we choose only data points satisfying Eq. (6) for a fixed constant c , the corresponding extrapolation would suppress both physical and algorithmic errors and also be more data-efficient than the previously proposed two-dimensional extrapolation.

The error rate of the global depolarizing noise could be related to that of the local stochastic noise. Suppose that a quantum circuit with N quantum gates. Assuming that the local stochastic noise $\mathcal{N}_{\text{local}}$ that acts on a quantum state with probability p_{local} occurs after each quantum gate. Then, the probability that a quantum state is not affected by all of the local noise channels per depth would be approximated by $1 - Np_{\text{local}}$. Thus, given that all of the local noise channels in a quantum circuit are modeled by one global depolarizing noise, the error rate of global depolarizing noise p_{global} is $\mathcal{O}(Np_{\text{local}})$.

By analyzing the Trotter error shown in Eq. (9) or a tighter bound [31], we can reduce a more fine-grained optimal Trotter number. For example, let us consider the dynamics of a 1D transverse-field Ising model

$$H_{1\text{D TFI}} = J \sum_{i=1}^n Z_i Z_{i+1} + B \sum_{i=1}^n X_i,$$

where we set $Z_{n+1} = Z_1$. Using the tighter 1st Trotter error with commutator scaling [31], we obtain

$$\left\| U_{\text{targ}}^{\frac{1}{M}} - U_{\text{TR}} \right\|_{\text{op}} \leq 2|J||B|n \frac{t^2}{M^2},$$

where $\|A\|_{\text{op}}$ is the spectral norm of A . From this inequality, we expect that $D(\mathcal{U}_{\text{targ}}, \mathcal{U}_{\text{TR}}) \leq \tilde{a}|J||B|n \frac{t^2}{M^2}$ for a constant \tilde{a} . Combining this inequality with $D(\mathcal{E}_{\text{TR}}, \mathcal{U}_{\text{TR}}) \propto p_{\text{global}}$, we get

$$M_{\text{opt}} = \mathcal{O}\left(|t| \sqrt{\frac{|J||B|n}{p_{\text{global}}}}\right).$$

If we assume $p_{\text{global}} = \mathcal{O}(np_{\text{local}})$, we obtain

$$M_{\text{opt}} = \text{floor}\left(f|t| \sqrt{\frac{|J||B|}{p_{\text{local}}}}\right), \quad (7)$$

where f is a positive constant. In Sec. D, we discuss the validity of the above equation by numerically analyzing the scaling of the optimal Trotter number as a function of the simulation time.

We can also calculate the scaling of the optimal Trotter steps in the case of the 2D TFI Hamiltonian:

$$H_{2\text{D TFI}} = J \sum_{i \neq j} Z_i Z_j + B \sum_i X_i,$$

where we consider the periodic conditions. If we consider the $n \times n$ square lattice, the 1st Trotter error with commutator scaling of the 2D TFI can be obtained as

$$\left\| U_{\text{targ}} - U_{\text{TR}} \right\|_{\text{op}} \leq 4|J||B|n^2 \frac{t^2}{M^2}.$$

Thus, the optimal Trotter step can be given by

$$M_{\text{opt}} = \mathcal{O}\left(|t| \sqrt{\frac{|J||B|}{p_{\text{global}}}}\right).$$

B. Extrapolation Method using Optimal Trotter Number

Now, we provide a data-efficient extrapolation method for both errors using Eq. (6), which we dub data-efficient 1D extrapolation. Let ρ_0 be the initial state of the quantum circuit shown in Fig. 1. The output state of the quantum circuit can be given by

$$\begin{aligned} \rho(M, p_{\text{global}}) = & (1 - p_{\text{global}})^M [U_{\text{TR}}^M](\rho_0) \\ & + \left\{ 1 - (1 - p_{\text{global}})^M \right\} \frac{I^{\otimes n}}{2^n}. \end{aligned} \quad (8)$$

According to Ref. [4, 32], the first-order Trotterization can approximate a target time evolution unitary as

$$U_{\text{targ}} = U_{\text{TR}}^M + \frac{t^2}{2M} \sum_{i < j} [H_i, H_j] + \sum_{m=3}^{\infty} E(m),$$

where $E(m)$ can be upper-bounded by

$$\|E(m)\|_{\text{op}} \leq M \left\| \frac{Ht}{M} \right\|_{\text{op}}^m \frac{1}{m!}. \quad (9)$$

Then, we can rewrite the Trotterization as

$$U_{\text{TR}}^M = U_{\text{targ}} - \frac{t^2}{2M} h_{\text{comm}} - \sum_{m=3}^{\infty} E(m),$$

where $h_{\text{comm}} := \sum_{i < j} [H_i, H_j]$. Substituting the above equation into Eq. (8), we get

$$\begin{aligned} \rho(M, p_{\text{global}}) = & (1 - p_{\text{global}})^M \left(\rho_{\text{exact}} - \frac{t^2}{2M} \Delta + \frac{t^4}{4M^2} \eta - \kappa \right) \\ & + \left\{ 1 - (1 - p_{\text{global}})^M \right\} \frac{I^{\otimes n}}{2^n} + \mathcal{O}\left(\frac{1}{M^3}\right), \end{aligned}$$

where

$$\begin{aligned} \rho_{\text{exact}} &:= [U_{\text{targ}}](\rho_0), \quad \Delta := h_{\text{comm}} \rho_0 U_{\text{targ}}^{\dagger} + \text{h.c.} \\ \eta &:= [h_{\text{comm}}](\rho_0), \quad \kappa := \sum_{m=3}^{\infty} E(m) \rho_0 U_{\text{targ}}^{\dagger} + \text{h.c.} \end{aligned}$$

Here $\|\kappa\|_{\text{op}} = \mathcal{O}(p_{\text{global}})$. Using the Taylor expansion, $\rho(M, p_{\text{global}})$ for small p_{global} can be approximated by the following expression:

$$\begin{aligned} \rho(M, p_{\text{global}}) \approx & (1 - Mp_{\text{global}}) \left(\rho_{\text{exact}} - \frac{t^2}{2M} \Delta + \frac{t^4}{4M^2} \eta - \kappa \right) \\ & + Mp_{\text{global}} \frac{I^{\otimes n}}{2^n} + \mathcal{O}\left(\frac{1}{M^3}\right). \end{aligned}$$

Substituting Eq. (6) into the above expression and considering Eq. (9), we have

$$\begin{aligned} \rho(p_{\text{global}}) = & \rho_{\text{exact}} + p_{\text{global}}^{\frac{1}{2}} \left(c \frac{I^{\otimes n}}{2^n} - c \rho_{\text{exact}} - \frac{t^2}{2c} \Delta \right) \\ & + p_{\text{global}} \left(\frac{t^2}{2} \Delta + \frac{t^4}{4c^2} \eta - \frac{\kappa}{p_{\text{global}}} \right) \\ & + \mathcal{O}\left(p_{\text{global}}^{\frac{3}{2}}\right). \end{aligned} \quad (10)$$

Here, $p_{\text{global}}^{-1} \|\kappa\|_{\text{op}} = \mathcal{O}(1)$. Thus, from Eq. (10), $\rho(p_{\text{global}})$ is expected to be expanded as a Taylor series in $p_{\text{global}}^{\frac{1}{2}}$, and we expect that the expectation value of an observable A for $\rho(p_{\text{global}})$ is given by

$$\langle A \rangle (p_{\text{global}}) = \langle A \rangle (0) + \sum_{i=1}^m A_i p_{\text{global}}^{\frac{i}{2}} + \mathcal{O}\left(p_{\text{global}}^{\frac{m+1}{2}}\right), \quad (11)$$

where A_i are the real coefficients. As in a standard polynomial extrapolation, by using $m+1$ different noisy expectation values $\{\langle A \rangle (\lambda_i p_{\text{global}})\}_{i=0}^m$ with $1 = \lambda_0 < \lambda_1 < \dots < \lambda_m$ and considering the polynomial of degree m in $p_{\text{global}}^{\frac{1}{2}}$ in Eq. (11), the estimator of this polynomial extrapolation is given by

$$\langle A \rangle_{\text{est}} = \sum_{i=0}^m g_i \langle A \rangle (\lambda_i p_{\text{global}}) + \mathcal{O}\left(p_{\text{global}}^{\frac{m+1}{2}}\right), \quad (12)$$

where

$$g_i := \prod_{j \neq i} \frac{\sqrt{\lambda_j}}{\sqrt{\lambda_j} - \sqrt{\lambda_i}}. \quad (13)$$

We dub this extrapolation as data-efficient 1D extrapolation.

IV. TROTTER SUBSPACE EXPANSION

Here, we propose Trotter subspace expansion that robustly mitigates both algorithmic and physical errors more than the proposed data-efficient extrapolation method at the cost of measurements. The Trotter subspace expansion is the combination of the proposed data-efficient extrapolation method and the purification methods, which certifies the physicality of the estimated result (See Sec. B).

We prepare the $n'+1$ output states of noisy Trotterized circuit $\sigma_i = \rho(p_i, M_i)$ ($i = 0, \dots, n'$), where $p_i = \lambda_i p_{\text{global}}$ with $1 = \lambda_0 < \lambda_1 < \dots < \lambda_{n'}$ and M_i are the error rates of physical noise and the Trotter number of the noisy Trotterized circuit, respectively. M_i is determined by Eq. (6) with a given constant factor c . Then, we virtually

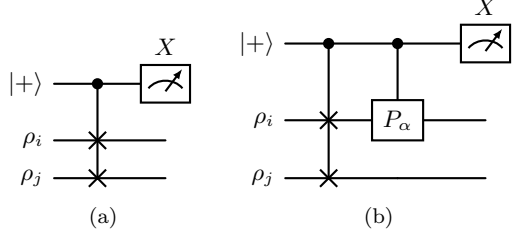


FIG. 2. Quantum circuits using the standard purification [20–22, 33] for evaluating the expectation value of an observable P_α for the ansatz state of the Trotter subspace ρ_{QEM} shown in Eq. (14). (a): Swap test circuit to evaluate $\text{Tr}(\rho_i \rho_j)$. This circuit allows us to evaluate $\text{Tr}(\rho_i \rho_j)$ by measuring the Pauli X of the most upper line. (b): Quantum circuit to evaluate $\text{Tr}(\rho_i \rho_j P_\alpha)$ by measuring the Pauli X , where $A = \sum_\alpha c_\alpha P_\alpha$ and P_α is a Pauli operator.

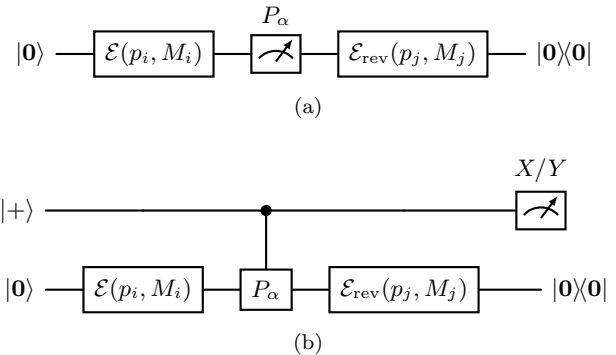


FIG. 3. Quantum circuits using the dual state purification [23, 34, 35] (a) and (b) for evaluating the expectation value of an observable P_α for the ansatz state of the Trotter subspace shown in Eqs. (16) and (17), respectively.

construct the following state:

$$\begin{aligned} \rho_{\text{TS}} &= \sum_{i=0}^{n'} g_i \rho_i, \\ \rho_{\text{QEM}} &= \frac{\rho_{\text{TS}}^2}{\text{Tr}(\rho_{\text{TS}}^2)}, \end{aligned} \quad (14)$$

where $\rho_i := \rho(p_i, M_i)$ and g_i is determined by Eq. (13). The ansatz state ρ_{QEM} satisfies $\text{Tr}(\rho_{\text{QEM}}) = 1$ and $\rho \geq 0$, which ensures that ρ_{QEM} is physical. Then, the corresponding error-mitigated expectation value of A is given by

$$\langle A \rangle_{\text{est}} = \frac{\sum_{i,j=0}^{n'} g_i g_j \text{Tr}(\rho_i \rho_j A)}{\sum_{i,j=0}^{n'} g_i g_j \text{Tr}(\rho_i \rho_j)}. \quad (15)$$

To obtain each term constituting $\langle A \rangle_{\text{est}}$, i.e., $\text{Tr}(\rho_i \rho_j A)$ and $\text{Tr}(\rho_i \rho_j)$ in Eq. (15), we use a modified quantum circuit of purification-based QEM methods. The quantum circuits for Trotter subspace expansion for copy-based purification are shown in Fig. 2 [33] (see Sec. C for more details).

In summary, we can perform the Trotter subspace expansion in the following procedure:

1. Choose the $n' + 1$ parameter pairs (p_i, M_i) , composed of the physical error rate p_i and Trotter number M_i , where M_i is determined by Eq. (6). Then, prepare the corresponding noisy Trotterized quantum circuit $\mathcal{C}(p_i, M_i)$.
2. For $i, j = 0, \dots, n'$, repeat the following operations.
 - (a) Using the quantum circuits $\mathcal{C}(p_i, M_i)$ and $\mathcal{C}(p_j, M_j)$, prepare the output states $\rho_i := \rho(p_i, M_i)$ and ρ_j as the initial states for the quantum circuits shown in Fig. 2.
 - (b) Obtain $\text{Tr}(\rho_i \rho_j)$ and $\text{Tr}(\rho_i \rho_j A)$ using the quantum circuits shown in Figs. 2a and 2b.
3. Calculate the coefficients g_i by Eq. (13).
4. Calculate the denominator and the numerator in Eq. (15) and then output the estimator $\langle A \rangle_{\text{est}}$.

To circumvent the use of copies in our method, we can use a dual-state purification circuit [23, 34, 35]. By the dual-state purification, we can compute the expectation values for following error-mitigated states:

$$\rho_{\text{Dual}}^{(1)} = \frac{\rho_{\text{TS}} \bar{\rho}_{\text{TS}} + \bar{\rho}_{\text{TS}} \rho_{\text{TS}}}{2 \text{Tr}(\rho_{\text{TS}} \bar{\rho}_{\text{TS}})} \quad (16)$$

or

$$\rho_{\text{Dual}}^{(2)} = \frac{\rho_{\text{TS}} \bar{\rho}_{\text{TS}}}{\text{Tr}(\rho_{\text{TS}} \bar{\rho}_{\text{TS}})} \quad (17)$$

with $\bar{\rho}_{\text{TS}} = \sum_i g_i \bar{\rho}_i$, where $\bar{\rho}_i := \bar{\rho}(p_i, M_i)$. Figure 3 shows the quantum circuits for evaluating each term comprising the expectation values for the error-mitigated state in Eqs. (16) and (17) [35]. For $\rho_{\text{Dual}}^{(1)}$, we need to compute $\text{Tr}(\rho_i \bar{\rho}_j)$ and $\frac{1}{2} \text{Tr}((\rho_i \bar{\rho}_j + \bar{\rho}_i \rho_j) A)$. Figures 3a and 3b shows the quantum circuit for computing those terms for intermediate measurement and indirect measurement methods. For $\rho_{\text{Dual}}^{(2)}$, we need to measure $\text{Tr}(\rho_i \bar{\rho}_j A)$, which can be evaluated by measuring the Pauli Y operator in the indirect measurement method and computing $\langle X \rangle - i \langle Y \rangle$ (See Sec. C for more details). Because the dual state $\bar{\rho}$ well-approximate the original state ρ for a deep circuit under the stochastic Pauli noise [35], both $\rho_{\text{Dual}}^{(1)}$ and $\rho_{\text{Dual}}^{(2)}$ can be employed as a good approximation of the purified state ρ_{QEM} in Eq. (14) in this case.

V. NUMERICAL SIMULATION

In this section, we present numerical simulations of the Trotter subspace expansion applied to the one-dimensional transverse Ising model. We initialize the

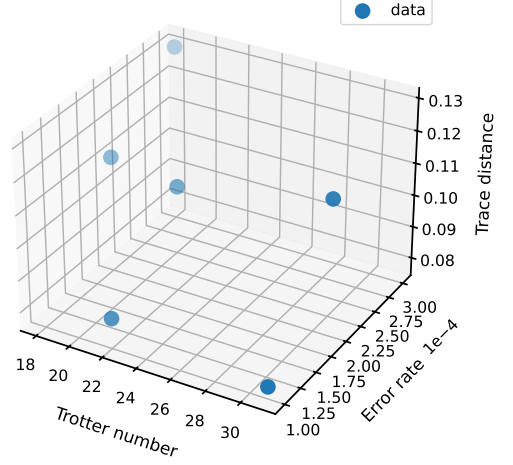


FIG. 4. Trace distance between an output state of a noisy Trotterized quantum circuit used for our numerical simulation and the exact state. In our numerical simulation, we set the total simulation time as $t = 1$ and the physical error rates as $p_1 = 1.0 \times 10^{-5}$. We use the output states such that the corresponding quantum circuits are parametrized by $(p_2, M) = (2 \times 10^{-4}, 18), (3 \times 10^{-4}, 18), (1 \times 10^{-4}, 22), (2 \times 10^{-4}, 22), (1 \times 10^{-4}, 31)$, and $(2 \times 10^{-4}, 31)$. The raw data and the VD use the output state where $(p_2, M) = (1 \times 10^{-4}, 31)$, whose trace distance is the smallest. The previous methods use all of the output states, whereas our proposed data-efficient extrapolation uses only the three output states where $(p_2, M) = (3 \times 10^{-4}, 18), (2 \times 10^{-4}, 22)$, and $(1 \times 10^{-4}, 18)$, satisfying Eq. (6). Our proposed Trotter subspace expansion also uses all of the output states, but the number of the required circuits to calculate its estimator is more than those of the previous methods.

system in the zero state $|0 \dots 0\rangle$ and simulate the time evolution under the Hamiltonian

$$H_{\text{TFI}} = - \sum_{i=1}^n Z_i Z_{i+1} + \sum_{i=1}^n X_i,$$

where n denotes the number of qubits and we set $Z_{n+1} = Z_1$. We approximate the time evolution under this Hamiltonian by the first-order Trotterization:

$$U_{\text{Trotter}} = \left\{ \exp \left(i \sum_{i=1}^n Z_i Z_{i+1} \frac{t}{M} \right) \exp \left(-i \sum_{i=1}^n X_i \frac{t}{M} \right) \right\}^M.$$

In our simulation, we set $n = 10$ and $t = 1$, and we assume that there is single- or two-qubit depolarizing noise after a single- or two-qubit gate, respectively. The single-qubit depolarizing noise that acts on qubit k is defined as

$$\mathcal{N}_{\text{1-qubit depo } k}(\rho) = (1 - p_1) \rho + \frac{p_1}{2} I_k \otimes \text{Tr}_k(\rho),$$

and the two-qubit depolarizing noise that acts on qubit k and qubit l is defined as

$$\mathcal{N}_{\text{2-qubit depo } k, l}(\rho) = (1 - p_2) \rho + \frac{p_2}{4} I_{k,l} \otimes \text{Tr}_{k,l}(\rho).$$

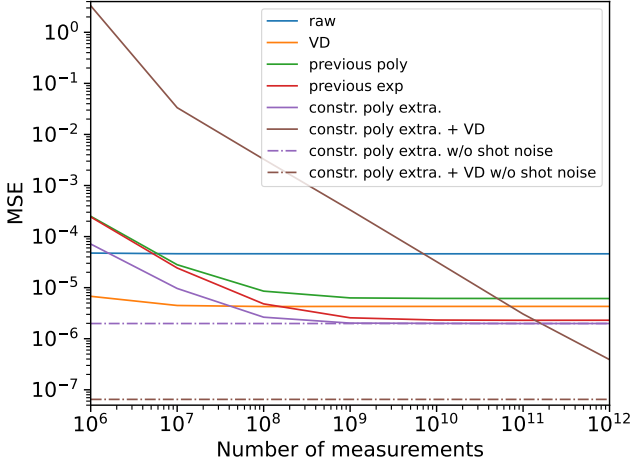


FIG. 5. Benchmark of QEM methods depending on the number of measurements. We estimate the expectation value of an observable X_1 for a time-evolved state of the 1D transverse Ising model and calculate the mean squared error (MSE) as a function of the number of measurements. The blue, orange, green, red, purple, and brown solid lines stand for the statistics considering shot noise from raw data, VD, the previous method using the polynomial extrapolation in terms of physical noise, the previous method using the exponential extrapolation in terms of physical noise, our proposed data-efficient extrapolation, and the combination of the data-efficient extrapolation with VD, respectively. The purple and brown dashed-dotted lines represent the statistics without shot noise from our proposed data-efficient extrapolation and the combination of the data-efficient extrapolation with VD, respectively.

Here, ρ is an n -qubit state, and I_k and $I_{k,l}$ are the identity channel for qubit k and that for qubit k and qubit l , respectively. We set the physical error rates as $p_1 = 1.0 \times 10^{-5}$ and $p_2 \in \{1.0 \times 10^{-4}, 2.0 \times 10^{-4}, 3.0 \times 10^{-4}\}$, respectively. By using Eq. (6) with $p_{\text{global}} = np_2$ and $c = 1$, we determine the Trotter number to be $M \in \{18, 22, 31\}$.

We benchmark the finite shot noise effect for QEM methods, including our estimators. We compare our proposed two methods, the 1D data-efficient extrapolation Eq. (12) and the Trotter subspace expansion Eq. (15), with other QEM methods such as virtual distillation (VD) [20, 22] and the previous methods, i.e., the sequential physical and Trotter error extrapolation using a physical polynomial or exponential extrapolation [19]. Note that we do not consider quantum noise in the purification circuits for the VD and the Trotter subspace expansion shown in Fig. 2 for simplicity.

In Fig. 4, we plot the trace distance between the exact time-evolved state and an output state of a noisy Trotterized quantum circuit used for our numerical simulation. We use the output states such that the corresponding quantum circuits are parametrized by $(p_2, M) = (2 \times 10^{-4}, 18), (3 \times 10^{-4}, 18), (1 \times 10^{-4}, 22)$,

$(2 \times 10^{-4}, 22)$, $(1 \times 10^{-4}, 31)$, and $(2 \times 10^{-4}, 31)$. The raw data and the VD use the output state where $(p_2, M) = (1 \times 10^{-4}, 31)$, whose trace distance is the smallest. The previous methods use all of the output states, whereas our proposed data-efficient extrapolation uses only the three output states where $(p_2, M) = (3 \times 10^{-4}, 18), (2 \times 10^{-4}, 22)$, and $(1 \times 10^{-4}, 18)$, satisfying Eq. (6). Our proposed Trotter subspace expansion also uses all of the output states, but the number of the required circuits to calculate its estimator is more than those of the previous methods.

To see the effect of the finite number of measurements, we calculate the mean squared error (MSE) of each estimator:

$$\text{MSE} = (\langle A \rangle_{\text{exact}} - \langle A \rangle_{\text{est}})^2.$$

We plot the MSE of each estimator as a function of the number of measurements N shown in Fig. 5.

From Fig. 5, we find that the MSE of the data-efficient extrapolation is the least in the QEM methods if $10^8 \leq N \leq 10^{11}$. At 10^8 measurements, we see that the MSE of the data-efficient extrapolation is 17.5 times smaller than the noisy result, 1.6 times smaller than the VD, and 1.8 times smaller than the previous method using the exponential extrapolation in terms of physical noise. Also, the converged MSE of the data-efficient extrapolation is 23 times smaller than the noisy result, 2.2 times smaller than the VD, and 1.2 times smaller than the previous method using the exponential extrapolation in terms of physical noise. Thus, the data-efficient extrapolation would be more helpful than the previous methods and the VD.

As for the Trotter subspace expansion, we see that, if we use at least 10^{12} measurements, the MSE of the Trotter subspace expansion is the least among the QEM methods. Also, the converged MSE of the Trotter subspace expansion is 710 times smaller than the raw data, and 31 times smaller than the data-efficient extrapolation. Thus, if we can execute many quantum computers in parallel, the Trotter subspace expansion would be more useful than the other QEM methods.

VI. CONCLUSION

We have presented two error mitigation methods for noisy Trotterized quantum circuits that suppress both physical and algorithmic errors: the data-efficient 1D extrapolation and the Trotter subspace expansion. The data-efficient 1D extrapolation, which uses the output states parametrized by only one parameter: an error rate of physical noise. The key point of this method is that it uses the expectation values satisfying the scaling of the optimal Trotter number with respect to a physical error rate, thereby mitigating both algorithmic and physical errors with fewer expectation values than the previous methods [19]. Then, we proposed the Trotter subspace expansion, i.e., the combination of the data-efficient 1D

extrapolation and the VD. In addition, we have discussed how to implement the Trotter subspace expansion with fewer copies of quantum states by using dual-state purification.

The data-efficient 1D extrapolation is better than the previous methods in terms of the MSE for almost all the measurement shots in our numerical simulation. The converged MSE of the data-efficient extrapolation is 1.2 times smaller than the previous method using the physical error exponential extrapolation. We expect that the twirling, such as a symmetry Clifford twirling [36], approximates the quantum noise as the global depolarizing noise, making our proposed extrapolation method more effective.

Moreover, we have numerically seen that the Trotter subspace expansion can be more accurate than the previous methods if we use at least 10^{12} measurements. Its converged MSE is 710 times smaller than the raw data and 31 times smaller than the data-efficient extrapolation. Thus, the Trotter subspace expansion would be more useful than the other QEM methods if we can execute many quantum computers in parallel.

Our work leaves several open questions. Although we have considered the first-order deterministic Trotterization, it can be extended to the higher-order Trotterization [5, 37] or randomized Trotterization [6, 38]. Recently, post-Trotter methods, such as truncated Taylor series [7–9] and quantization [10], have been proposed, and such methods exponentially improve as a function of the desired accuracy compared to the Trotter ones [3].

We also expect that one could give the extension of our work or invention for the post-Trotter methods. It would be interesting to apply our proposed method to the statistical phase estimation [26], which is one of the most promising algorithms for the early-fault tolerant era. Finally, it may be interesting to seek whether our subspace Trotter expansion is helpful in activating the entanglement for quantum metrology [39].

Note added—. When we are finalizing the manuscript, we became aware of a similar work discussing a one-dimensional extrapolation method for both algorithmic and physical errors [40]. While their work considers the continuous time evolution model for a noisy second-order Trotter algorithm and adopts a similar parameter tuning to $p \propto M^{-2}$, they do not argue the reason for the optimality of the choice. Also, Xu *et. al.* [41] have proved that the physical and algorithmic errors in every noisy Trotter step decay exponentially with Trotter steps by the state-dependent analysis.

ACKNOWLEDGMENTS

This work was supported by JST [Moonshot R&D] Grant Nos. JPMJMS2061; JST, PRESTO, Grant No. JPMJPR2114, Japan; MEXT Q-LEAP, Grant Nos. JPMXS0120319794 and JPMXS0118068682; JST CREST Grant No. JPMJCR23I4.

[1] Y. Kim, A. Eddins, S. Anand, K. X. Wei, E. van den Berg, S. Rosenblatt, H. Nayfeh, Y. Wu, M. Zaletel, K. Temme, and A. Kandala, Evidence for the utility of quantum computing before fault tolerance, *Nature* **618**, 500 (2023).

[2] A. M. Childs, D. Maslov, Y. Nam, N. J. Ross, and Y. Su, Toward the first quantum simulation with quantum speedup, *Proc. Natl. Acad. Sci. U.S.A.* **115**, 9456 (2018).

[3] N. Yoshioka, T. Okubo, Y. Suzuki, Y. Koizumi, and W. Mizukami, Hunting for quantum-classical crossover in condensed matter problems, *npj Quantum Inf* **10**, 1 (2024).

[4] S. Lloyd, Universal Quantum Simulators, *Science* **273**, 1073 (1996).

[5] M. Suzuki, Generalized Trotter's formula and systematic approximants of exponential operators and inner derivations with applications to many-body problems, *Commun. Math. Phys.* **51**, 183 (1976).

[6] E. Campbell, Random Compiler for Fast Hamiltonian Simulation, *Phys. Rev. Lett.* **123**, 070503 (2019).

[7] D. W. Berry, A. M. Childs, R. Cleve, R. Kothari, and R. D. Somma, Exponential improvement in precision for simulating sparse Hamiltonians, in *Proceedings of the Forty-Sixth Annual ACM Symposium on Theory of Computing*, STOC '14 (Association for Computing Machinery, New York, NY, USA, 2014) pp. 283–292.

[8] D. W. Berry, A. M. Childs, R. Cleve, R. Kothari, and R. D. Somma, Simulating Hamiltonian Dynamics with a Truncated Taylor Series, *Phys. Rev. Lett.* **114**, 090502 (2015).

[9] R. Babbush, D. W. Berry, I. D. Kivlichan, A. Y. Wei, P. J. Love, and A. Aspuru-Guzik, Exponentially more precise quantum simulation of fermions in second quantization, *New J. Phys.* **18**, 033032 (2016).

[10] G. H. Low and I. L. Chuang, Hamiltonian Simulation by Qubitization, *Quantum* **3**, 163 (2019).

[11] K. Temme, S. Bravyi, and J. M. Gambetta, Error Mitigation for Short-Depth Quantum Circuits, *Phys. Rev. Lett.* **119**, 180509 (2017).

[12] Y. Li and S. C. Benjamin, Efficient Variational Quantum Simulator Incorporating Active Error Minimization, *Phys. Rev. X* **7**, 021050 (2017).

[13] S. Endo, S. C. Benjamin, and Y. Li, Practical Quantum Error Mitigation for Near-Future Applications, *Phys. Rev. X* **8**, 031027 (2018).

[14] Y. Suzuki, S. Endo, K. Fujii, and Y. Tokunaga, Quantum Error Mitigation as a Universal Error Reduction Technique: Applications from the NISQ to the Fault-Tolerant Quantum Computing Eras, *PRX Quantum* **3**, 010345 (2022).

[15] Y. Xiong, D. Chandra, S. X. Ng, and L. Hanzo, Sampling

Overhead Analysis of Quantum Error Mitigation: Uncoded vs. Coded Systems, *IEEE Access* **8**, 228967 (2020).

[16] C. Piveteau, D. Sutter, S. Bravyi, J. M. Gambetta, and K. Temme, Error Mitigation for Universal Gates on Encoded Qubits, *Phys. Rev. Lett.* **127**, 200505 (2021).

[17] M. Lostaglio and A. Ciani, Error Mitigation and Quantum-Assisted Simulation in the Error Corrected Regime, *Phys. Rev. Lett.* **127**, 200506 (2021).

[18] M. A. Wahl, A. Mari, N. Shammah, W. J. Zeng, and G. S. Ravi, Zero Noise Extrapolation on Logical Qubits by Scaling the Error Correction Code Distance, in *2023 IEEE International Conference on Quantum Computing and Engineering (QCE)* (IEEE, Bellevue, WA, USA, 2023) pp. 888–897.

[19] S. Endo, Q. Zhao, Y. Li, S. Benjamin, and X. Yuan, Mitigating algorithmic errors in a Hamiltonian simulation, *Phys. Rev. A* **99**, 012334 (2019).

[20] B. Koczor, Exponential Error Suppression for Near-Term Quantum Devices, *Phys. Rev. X* **11**, 031057 (2021).

[21] B. Koczor, The dominant eigenvector of a noisy quantum state, *New J. Phys.* **23**, 123047 (2021).

[22] W. J. Huggins, S. McArdle, T. E. O’Brien, J. Lee, N. C. Rubin, S. Boixo, K. B. Whaley, R. Babbush, and J. R. McClean, Virtual Distillation for Quantum Error Mitigation, *Phys. Rev. X* **11**, 041036 (2021).

[23] Z. Cai, Resource-efficient Purification-based Quantum Error Mitigation (2021), arXiv:2107.07279.

[24] D. Poulin and P. Wocjan, Sampling from the Thermal Quantum Gibbs State and Evaluating Partition Functions with a Quantum Computer, *Phys. Rev. Lett.* **103**, 220502 (2009).

[25] M. A. Nielsen and I. L. Chuang, *Quantum Computation and Quantum Information*, 10th ed. (Cambridge university press, Cambridge, 2010).

[26] L. Lin and Y. Tong, Heisenberg-Limited Ground-State Energy Estimation for Early Fault-Tolerant Quantum Computers, *PRX Quantum* **3**, 010318 (2022).

[27] G. C. Knee and W. J. Munro, Optimal Trotterization in universal quantum simulators under faulty control, *Physical Review A* **91**, 10.1103/PhysRevA.91.052327 (2015).

[28] A. Gilchrist, N. K. Langford, and M. A. Nielsen, Distance measures to compare real and ideal quantum processes, *Phys. Rev. A* **71**, 062310 (2005).

[29] D. Qin, Y. Chen, and Y. Li, Error statistics and scalability of quantum error mitigation formulas, *npj Quantum Inf* **9**, 1 (2023).

[30] K. Tsubouchi, T. Sagawa, and N. Yoshioka, Universal Cost Bound of Quantum Error Mitigation Based on Quantum Estimation Theory, *Phys. Rev. Lett.* **131**, 210601 (2023).

[31] A. M. Childs, Y. Su, M. C. Tran, N. Wiebe, and S. Zhu, Theory of Trotter Error with Commutator Scaling, *Phys. Rev. X* **11**, 011020 (2021).

[32] B. Sanders, G. Ahokas, R. Cleve, and D. Berry, Quantum Algorithms for Hamiltonian Simulation, in *Mathematics of Quantum Computation and Quantum Technology*, Vol. 20074453, edited by G. Chen, L. Kauffman, and S. Lomonaco (Chapman and Hall/CRC, 2007) pp. 89–112.

[33] N. Yoshioka, H. Hakoshima, Y. Matsuzaki, Y. Tokunaga, Y. Suzuki, and S. Endo, Generalized Quantum Subspace Expansion, *Phys. Rev. Lett.* **129**, 020502 (2022).

[34] M. Huo and Y. Li, Dual-state purification for practical quantum error mitigation, *Phys. Rev. A* **105**, 022427 (2022).

[35] B. Yang, N. Yoshioka, H. Harada, S. Hakkaku, Y. Tokunaga, H. Hakoshima, K. Yamamoto, and S. Endo, Resource-efficient generalized quantum subspace expansion, *Phys. Rev. Appl.* **23**, 054021 (2025).

[36] K. Tsubouchi, Y. Mitsuhashi, K. Sharma, and N. Yoshioka, Symmetric Clifford twirling for cost-optimal quantum error mitigation in early FTQC regime (2024), arXiv:2405.07720.

[37] J. D. Watson and J. Watkins, Exponentially Reduced Circuit Depths Using Trotter Error Mitigation (2024), arXiv:2408.14385.

[38] J. D. Watson, Randomly Compiled Quantum Simulation with Exponentially Reduced Circuit Depths (2025), arXiv:2411.04240.

[39] R. Trényi, Á. Lukács, P. Horodecki, R. Horodecki, T. Vértesi, and G. Tóth, Activation of metrologically useful genuine multipartite entanglement, *New J. Phys.* **26**, 023034 (2024).

[40] P. Mohammadipour and X. Li, Direct Analysis of Zero-Noise Extrapolation: Polynomial Methods, Error Bounds, and Simultaneous Physical-Algorithmic Error Mitigation (2025), arXiv:2502.20673.

[41] J. Xu, C. Zhao, J. Fan, and Q. Zhao, Exponentially Decaying Quantum Simulation Error with Noisy Devices (2025), arXiv:2504.10247.

[42] S. Endo, Z. Cai, S. C. Benjamin, and X. Yuan, Hybrid Quantum-Classical Algorithms and Quantum Error Mitigation, *J. Phys. Soc. Jpn.* **90**, 032001 (2021).

[43] Z. Cai, Quantum Error Mitigation using Symmetry Expansion, *Quantum* **5**, 548 (2021).

[44] A. Kandala, K. Temme, A. D. Córcoles, A. Mezzacapo, J. M. Chow, and J. M. Gambetta, Error mitigation extends the computational reach of a noisy quantum processor, *Nature* **567**, 491 (2019).

Appendix A: Review of quantum error mitigation methods

In this section, we briefly review the quantum error mitigation methods used in this paper: polynomial extrapolation method and virtual distillation. First, we review the error extrapolation method for physical errors. Then, we explain purification-based quantum error mitigation methods, which use multiple copies of noisy quantum states.

1. Error-extrapolation methods for physical errors

We review the polynomial error extrapolation according to Refs. [11, 12, 42, 43]. Suppose that we measure the expectation value of an observable A . We assume that there is one parameter for the physical error p in a quantum circuit. Expanding an expectation value of an observable $\langle A \rangle(p)$ up to the L th order, we obtain

$$\langle A \rangle(p) = \langle A \rangle(0) + \sum_{i=1}^L A_i p^i + \mathcal{O}(p^{L+1}), \quad (\text{A1})$$

where A_i stand for the coefficients of the expansion. Considering the $L+1$ expectation values $\langle A \rangle(p_1), \dots, \langle A \rangle(p_L)$ and expanding them in the same way as in Eq. (A1), we have the following estimator for the polynomial extrapolation:

$$\langle A \rangle_{\text{est}}(0) = \sum_{i=0}^L \langle A \rangle(p_i) \prod_{j \neq i} \frac{p_j}{p_j - p_i}.$$

The variance of this estimator is given by

$$\text{Var}[\langle A \rangle_{\text{est}}(0)] = \sum_{i=0}^L \text{Var}[\langle A \rangle(p_i)] \left(\prod_{j \neq i} \frac{p_j}{p_j - p_i} \right)^2.$$

a. Exponential error extrapolation

It is pointed out that the exponential error extrapolation is more suitable than the polynomial error extrapolation if the number of quantum gates N_g is large and the error rate of quantum noise p is small. Suppose that all of the quantum gates suffer from the same quantum noise defined as

$$\mathcal{N} = (1-p)[I] + p\mathcal{D},$$

where $[A](\rho) := A\rho A^\dagger$ and \mathcal{D} stands for a noisy map. Then, the noisy quantum circuit can be represented as

$$\begin{aligned} \mathcal{E}_{\text{circ}} &= \prod_{i=1}^{N_g} \mathcal{N}_i \circ \mathcal{U}_i \\ &= \sum_{i=0}^{N_g} (1-p)^{N_g-i} p^i \sum_{j=1}^{\binom{N_g}{i}} \mathcal{G}_i^j, \end{aligned} \quad (\text{A2})$$

where \mathcal{U}_i stands for an ideal quantum gate and \mathcal{G}_i^j stands for one of the expansion with i errors. Denoting the average of \mathcal{G}_i^j as

$$\mathcal{G}_i = \frac{\sum_{j=1}^{\binom{N_g}{i}} \mathcal{G}_i^j}{\binom{N_g}{i}},$$

Eq. (A2) can be rewritten as

$$\mathcal{E}_{\text{circ}} = \sum_{i=0}^{N_g} (1-p)^{N_g-i} p^i \binom{N_g}{i} \mathcal{G}_i. \quad (\text{A3})$$

Since $(1-p)^{N_g-i} p^i \binom{N_g}{i}$ is the binomial distribution, if N_g is sufficiently large and p is sufficiently small satisfying $N_g p = \mathcal{O}(1)$, the binomial distribution can be approximated by the Poisson distribution $e^{-N_g p} \frac{(N_g p)^i}{i!}$. Thus, Eq. (A3) can also be approximated by

$$\mathcal{E}_{\text{circ}} \approx e^{-N_g p} \sum_{i=0}^{N_g} \frac{(N_g p)^i}{i!} \mathcal{G}_i. \quad (\text{A4})$$

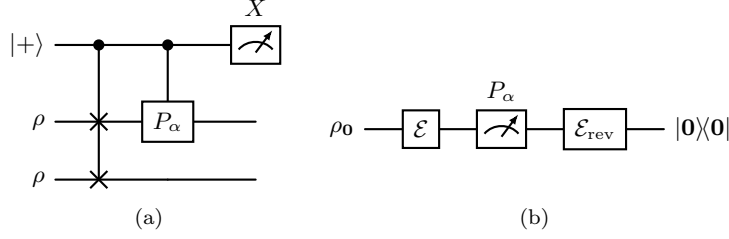


FIG. 6. Quantum circuits for purification-based QEM methods. (a): Copy-based purification. $\text{Tr}(P_\alpha \rho^2)$ can be obtained by the measurement of Pauli X of the most upper wire. (b): Dual-state purification with mid-circuit measurement. $\text{Tr}\left(\frac{\bar{\rho}\rho + \rho\bar{\rho}}{2} P_\alpha\right)$ can be obtained by mid-circuit measurement of Pauli operator P_α and then postselecting on the measurement outcome $\mathbf{0}$, where $\bar{\rho}$ is the dual state of ρ . $\text{Tr}\left(\frac{\bar{\rho}\rho + \rho\bar{\rho}}{2} P\right)$ is expected to be a good approximation of $\text{Tr}(P\rho^2)$.

From Eq. (A4), the noisy expectation values $\langle A \rangle(p)$ and $\langle A \rangle(rp)$ ($r > 1$) can be given by

$$\begin{aligned}\langle A \rangle(p) &= e^{-p} \langle A \rangle(0), \\ \langle A \rangle(rp) &= e^{-rp} \langle A \rangle(0).\end{aligned}$$

Thus, we have the following estimator for exponential extrapolation:

$$\langle A \rangle_{\text{est}}(0) = \langle A \rangle(p)^{\frac{r}{r-1}} \langle A \rangle(rp)^{\frac{1}{1-p}}$$

2. Purification-based quantum error mitigation

Purification-based QEM methods use several copies of noisy state ρ to obtain an expectation value of an observable for a "purified" state, and it is suited for mitigating stochastic errors [20–22]. This method simulates the purified state to estimate an expectation value at the cost of state copies or the circuit depth. Let A be an observable. Then, the estimator for the expectation value of A when using the purification-based QEM is given by

$$\langle A \rangle_{\text{est}} = \frac{\text{Tr}(\rho^L A)}{\text{Tr}(\rho^L)}.$$

The corresponding effective state could be written as

$$\rho_{\text{PB}} = \frac{\rho^L}{\text{Tr}(\rho^L)},$$

for the integer $L \geq 2$. Now, let the spectral decomposition of the noisy state denote $\rho = \sum_k p_k |\phi_k\rangle\langle\phi_k|$ ($p_0 \geq p_1 \geq \dots$), $\langle\phi_i|\phi_j\rangle = \delta_{ij}$. Then, we get

$$\rho^L = p_0^L \left\{ |\phi_0\rangle\langle\phi_0| + \sum_{k \geq 1} \left(\frac{p_k}{p_0}\right)^L |\phi_k\rangle\langle\phi_k| \right\},$$

which clearly shows the exponential suppression of the effect of subdominant eigenvectors. Because it has been shown that the dominant eigenvector well approximates the noiseless state in the presence of stochastic errors such as amplitude damping and stochastic Pauli errors, this method can mitigate stochastic errors efficiently [21, 22].

There are two types of implementations for the purification-based QEM: copy-based purification [20–22] and dual-state purification [23, 34, 35]. In the former purification protocol, we use copies of the quantum state. To measure $\text{Tr}(\rho^L P_\alpha)$ for a Pauli operator P_α for $L = 2$, we resort to the Hadamard test circuit in which the target unitary is the product of the swap operator and the observable of interest, as shown in Fig. 6a. Also, we can compute the denominator by using the circuit that removes the controlled- P_α operator from the circuit shown in Fig. 6a. See Refs. [20–22] for details.

Meanwhile, the dual-state purification method purifies the error-mitigated state with the doubled-depth quantum circuit as shown in Fig. 6b. Let the initial state denote $\rho_0 = |\mathbf{0}\rangle\langle\mathbf{0}|$, and let the process for the computation denote \mathcal{E}

that turns ρ_0 into $\rho = \mathcal{E}(\rho_0)$. We also introduce the uncomputational process \mathcal{E}_{rev} corresponding to \mathcal{E} . More precisely, \mathcal{E} and \mathcal{E}_{rev} are described as

$$\begin{aligned}\mathcal{E} &:= \mathcal{N}_L \circ \mathcal{U}_L \circ \cdots \circ \mathcal{N}_1 \circ \mathcal{U}_1, \\ \mathcal{E}_{\text{rev}} &:= \mathcal{N}_1^{(\text{rev})} \circ \mathcal{U}_1 \circ \cdots \circ \mathcal{N}_L^{(\text{rev})} \circ \mathcal{U}_L,\end{aligned}$$

where \mathcal{U}_k denotes an error-free quantum gate process, and \mathcal{N}_k or $\mathcal{N}_k^{(\text{rev})}$ denotes the accompanying quantum noise process. Then, the estimator for the expectation value of A when using the dual-state purification is given by

$$\langle A \rangle_{\text{est}} = \frac{\text{Tr}\left(\frac{\rho\bar{\rho} + \bar{\rho}\rho}{2} A\right)}{\text{Tr}(\rho\bar{\rho})}.$$

Here, $\bar{\rho} := \mathcal{E}_{\text{rev}}(\rho_0) = \sum_i K_i^\dagger \rho_0 K_i$ is called the dual state, with $\mathcal{E}_{\text{rev}}(\sigma) = \sum_i K_i \sigma K_i^\dagger$. In the case without noise, we have $\rho = \bar{\rho}$, and thus it is highly likely the dual state is a good approximation of the state ρ ; furthermore, assuming that $\mathcal{N}_k = \mathcal{N}_k^{(\text{rev})}$ for all k , it has been numerically shown that the trace distance of ρ and $\bar{\rho}$ becomes small under stochastic Pauli noise as the depth of the quantum circuit increases [35].

We evaluate the joint probability of measuring the $x \in \{0, 1\}$ in the mid-circuit measurement and measuring all the qubits in 0 at the final measurement. The joint probability reads $p_{x,0} = \text{Tr}\left[\mathcal{E}_{\text{rev}}\left(\frac{I + (-1)^x P_a}{2}\right) \mathcal{E}(\rho_0) \frac{I + (-1)^x P_a}{2}\right] P_0$ for the initial state $\rho_0 = |0\rangle\langle 0|$ and the projector onto the initial state $P_0 = |0\rangle\langle 0|$. Then, we can show

$$p_{0,0} - p_{1,0} = \text{Tr}\left(\frac{\bar{\rho}\rho + \rho\bar{\rho}}{2} P_a\right).$$

Thus, we can evaluate the numerator. Also, by removing the mid-circuit measurement from the circuit shown in Fig. 6b, we can evaluate the denominator by estimating the probability of measuring all the qubits in 0. Indeed, the probability is given by

$$p_0 = \text{Tr}[\mathcal{E}_{\text{rev}}(\mathcal{E}(\rho_0)) P_0] = \text{Tr}(\rho\bar{\rho}).$$

Appendix B: General remarks of error-extrapolation methods

Error extrapolation methods are relatively easier to implement than the other QEM methods, and thus, various experiments have been conducted [1, 44]. However, the effective state of an error extrapolation method may not be physical in general, which may cause bias. For example, consider the following estimator of extrapolation methods:

$$\begin{aligned}\langle A \rangle_{\text{est}} &= \sum_i c_i \langle A \rangle(p_i) \\ &= \sum_i c_i \text{Tr}(\rho(p_i) A).\end{aligned}\tag{B1}$$

The error extrapolation methods, such as the polynomial extrapolation and the exponential extrapolation, can be written in the above form. From Eq. (B1), the corresponding effective state could be written as

$$\rho_{\text{extra}} = \sum_i c_i \rho_i.$$

In general, ρ_{extra} could not satisfy $\rho \geq 0$.

An estimated expectation value using an unphysical state may cause a large bias. Consider an expectation value of an observable A for a general operator ρ . The expectation value can be bounded by the following inequality:

$$|\text{Tr}(A\rho)| \leq |\rho|_{\text{op}} \text{Tr}(|A|),\tag{B2}$$

where $|\cdot|_{\text{op}}$ is the operator norm, i.e., the maximum singular value of the operator A . If ρ is a density operator, $|\rho|_{\text{op}} \leq 1$, and thus we obtain

$$|\text{Tr}(A\rho)| \leq \text{Tr}(|A|).\tag{B3}$$

From Eq. (B3), we see that the absolute value of an estimated expectation value for a physical state is upper-bounded by the trace norm of A and independent of ρ . However, from Eq. (B2), if ρ is an unphysical state and has a large negative eigenvalue, the absolute value could be larger than the trace norm of A .

Appendix C: Quantum circuits for Trotter subspace expansion

In this section, we explain how the expectation value of an observable $A = \sum_{\alpha} c_{\alpha} P_{\alpha}$ for the ansatz state of the Trotter subspace expansion can be evaluated in detail. First, we show the evaluation method using the standard purification method, i.e., virtual distillation. Then, we explain the evaluation methods using dual-state purification methods, which require half the quantum states of the standard purification method at the expense of the circuit depth.

1. Standard purification method

In the case of the standard purification method, we adopt the ansatz state shown in Eq. (14). Recall that the expectation value of A for the ansatz state can be given by

$$\langle A \rangle_{\text{est}} = \frac{\sum_{i,j=0}^{n'} g_i g_j \text{Tr}(\rho_i \rho_j A)}{\sum_{i,j=0}^{n'} g_i g_j \text{Tr}(\rho_i \rho_j)} = \frac{\sum_{\alpha} c_{\alpha} \sum_{i,j=0}^{n'} g_i g_j \text{Tr}(\rho_i \rho_j P_{\alpha})}{\sum_{i,j=0}^{n'} g_i g_j \text{Tr}(\rho_i \rho_j)},$$

we have to evaluate the numerator and the denominator. To evaluate these expectation values, we review how the quantum circuits in Fig. 2 can measure $\text{Tr}(\rho_i \rho_j)$ and $\text{Tr}(\rho_i \rho_j P_{\alpha})$, where $\rho_i := \rho(p_i, M_i)$.

The expectation value of the Pauli X measurement in the circuit shown in Fig. 2a $\langle X \otimes I^{\otimes 2} \rangle$ is given by

$$\begin{aligned} \langle X \otimes I^{\otimes 2} \rangle_I &= \frac{1}{2} \text{Tr}(X \otimes I^{\otimes 2} |0\rangle\langle 1| \otimes \text{SWAP}(\rho_i \otimes \rho_j) + \text{h.c.}) \\ &= \text{Tr}(\rho_i \rho_j). \end{aligned} \quad (\text{C1})$$

From Eq. (C1), we find that the denominator can be estimated by the circuit shown in Fig. 2a.

The expectation value of the Pauli X measurement in the circuit shown in Fig. 2b $\langle X \otimes I^{\otimes 2} \rangle$ is given by

$$\begin{aligned} \langle X \otimes I^{\otimes 2} \rangle_{P_{\alpha}} &= \frac{1}{2} \text{Tr}(X \otimes P_{\alpha} \otimes I |0\rangle\langle 1| \otimes \text{SWAP}(\rho_i \otimes \rho_j) + \text{h.c.}) \\ &= \text{Tr}\left(\frac{\rho_i \rho_j + \rho_j \rho_i}{2} P_{\alpha}\right). \end{aligned} \quad (\text{C2})$$

On the other hand, the numerator of $\langle A \rangle_{\text{est}}$ can be rewritten as

$$\begin{aligned} \sum_{\alpha} c_{\alpha} \sum_{i,j=0}^{n'} g_i g_j \text{Tr}(\rho_i \rho_j P_{\alpha}) &= \sum_{\alpha} c_{\alpha} \left[\sum_{i=0}^{n'} g_i^2 \text{Tr}(\rho_i^2 P_{\alpha}) + \sum_{i < j} g_i g_j \{\text{Tr}(\rho_i \rho_j P_{\alpha}) + \text{Tr}(\rho_j \rho_i P_{\alpha})\} \right] \\ &= \sum_{\alpha} c_{\alpha} \left\{ \sum_{i=0}^{n'} g_i^2 \text{Tr}(\rho_i^2 P_{\alpha}) + 2 \sum_{i < j} g_i g_j \text{Tr}\left(\frac{\rho_i \rho_j + \rho_j \rho_i}{2} P_{\alpha}\right) \right\}. \end{aligned} \quad (\text{C3})$$

Combining Eq. (C2) with Eq. (C3), we find that both $\text{Tr}(\rho_i^2 P_{\alpha})$ and $\text{Tr}\left(\frac{\rho_i \rho_j + \rho_j \rho_i}{2} P_{\alpha}\right)$ can be estimated by the circuit shown in Fig. 2b, and thus the numerator can also be estimated by the circuit.

2. Dual-state purification method

In the case of the dual-state purification method, there are two choices of the ansatz states: $\rho_{\text{Dual}}^{(1)}$ and $\rho_{\text{Dual}}^{(2)}$ defined as Eqs. (16) and (17). After reviewing the measurement outcomes of the quantum circuits in Fig. 3, we explain how we can evaluate the expectation value of an observable $A = \sum_{\alpha} c_{\alpha} P_{\alpha}$ for such an ansatz state.

Figure 3a shows the quantum circuit for the Trotter subspace expansion using the dual-state purification with the mid-circuit measurement. In this circuit, we execute the mid-circuit measurement and then post-select the output state on the measurement outcome **0**. Let $p_{x,0}$ be the joint probability of measuring $x \in \{0, 1\}$ in the mid-circuit

measurement. The joint probability $p_{x,\mathbf{0}}$ is

$$\begin{aligned} p_{x,\mathbf{0}} &= \text{Tr} \left[\mathcal{E}_{\text{rev } j} \left(\frac{I + (-1)^x P_a}{2} \mathcal{E}_i(\rho_0) \frac{I + (-1)^x P_a}{2} \right) P_0 \right] \\ &= \text{Tr} \left[\frac{I + (-1)^x P_a}{2} \rho_i \frac{I + (-1)^x P_a}{2} \bar{\rho}_j \right], \end{aligned} \quad (\text{C4})$$

where $\mathcal{E}_{\text{rev } j} := \mathcal{E}_{\text{rev}}(p_j, M_j)$, $\mathcal{E}_i := \mathcal{E}(p_i, M_i)$, $\rho_0 := |\mathbf{0}\rangle\langle\mathbf{0}|$, and $P_0 := |\mathbf{0}\rangle\langle\mathbf{0}|$. From Eq. (C4), we obtain the following equation:

$$p_{0,\mathbf{0}} - p_{1,\mathbf{0}} = \text{Tr} \left(\frac{\rho_i \bar{\rho}_j + \bar{\rho}_j \rho_i}{2} P_\alpha \right). \quad (\text{C5})$$

Also, by removing the mid-circuit measurement from the circuit shown in Fig. 3a, the probability of measuring all the qubits in 0 is given by

$$p_0 = \text{Tr}(\rho_i \bar{\rho}_j). \quad (\text{C6})$$

Figure 3b shows the quantum circuit for the Trotter subspace expansion using the dual-state purification with the indirect measurement. The measurement outcomes become

$$\begin{aligned} \langle X \otimes P_0 \rangle &= \frac{1}{2} \{ \text{Tr}(\mathcal{E}_{\text{rev } j}(\mathcal{E}_i(\rho) P_\alpha) |\mathbf{0}\rangle\langle\mathbf{0}|) + \text{Tr}(\mathcal{E}_{\text{rev } j}(P_\alpha \mathcal{E}_i(\rho)) |\mathbf{0}\rangle\langle\mathbf{0}|) \} = \text{Tr} \left(\frac{\rho_i \bar{\rho}_j + \bar{\rho}_j \rho_i}{2} P_\alpha \right), \\ \langle Y \otimes P_0 \rangle &= \frac{1}{2} \{ -i \text{Tr}(\mathcal{E}_{\text{rev } j}(\mathcal{E}_i(\rho) P_\alpha) |\mathbf{0}\rangle\langle\mathbf{0}|) + i \text{Tr}(\mathcal{E}_{\text{rev } j}(P_\alpha \mathcal{E}_i(\rho)) |\mathbf{0}\rangle\langle\mathbf{0}|) \} = i \text{Tr} \left(\frac{\rho_i \bar{\rho}_j - \bar{\rho}_j \rho_i}{2} P_\alpha \right). \end{aligned} \quad (\text{C7})$$

Combining these results, we see that

$$\langle X \otimes P_0 \rangle - i \langle Y \otimes P_0 \rangle = \text{Tr}(\rho_i \bar{\rho}_j P_\alpha). \quad (\text{C8})$$

$$a. \quad \rho_{\text{Dual}}^{(1)}$$

The expectation value of an observable for $\rho_{\text{Dual}}^{(1)}$ is given by

$$\langle A \rangle_{\text{est}} = \frac{\sum_\alpha c_\alpha \sum_{i,j} g_i g_j \text{Tr} \left(\frac{\rho_i \bar{\rho}_j + \bar{\rho}_j \rho_i}{2} P_\alpha \right)}{\sum_{i,j} \text{Tr}(\rho_i \bar{\rho}_j)}.$$

According to Eqs. (C5) and (C7), the numerator can be estimated by the circuit using the mid-circuit measurement shown in Fig. 3a or the circuit using the indirect measurement shown in Fig. 3b. Also, from Eq. (C6), the denominator can be estimated by the circuit that removes the mid-circuit measurement from the one shown in Fig. 3a.

$$b. \quad \rho_{\text{Dual}}^{(2)}$$

The expectation value of an observable for $\rho_{\text{Dual}}^{(2)}$ is given by

$$\langle A \rangle_{\text{est}} = \frac{\sum_\alpha c_\alpha \sum_{i,j} g_i g_j \text{Tr}(\rho_i \bar{\rho}_j P_\alpha)}{\sum_{i,j} \text{Tr}(\rho_i \bar{\rho}_j)}.$$

According to Eq. (C8), the numerator can be estimated by the circuit using the indirect measurement shown in Fig. 3b. Note that we need to perform measurements of not only X but also Y on the ancilla qubit in this circuit, contrary to the case of $\rho_{\text{Dual}}^{(1)}$, where we only need to perform a measurement of X . Similar to the case of $\rho_{\text{Dual}}^{(1)}$, the denominator can be estimated by the circuit that removes the mid-circuit measurement from the one shown in Fig. 3a.

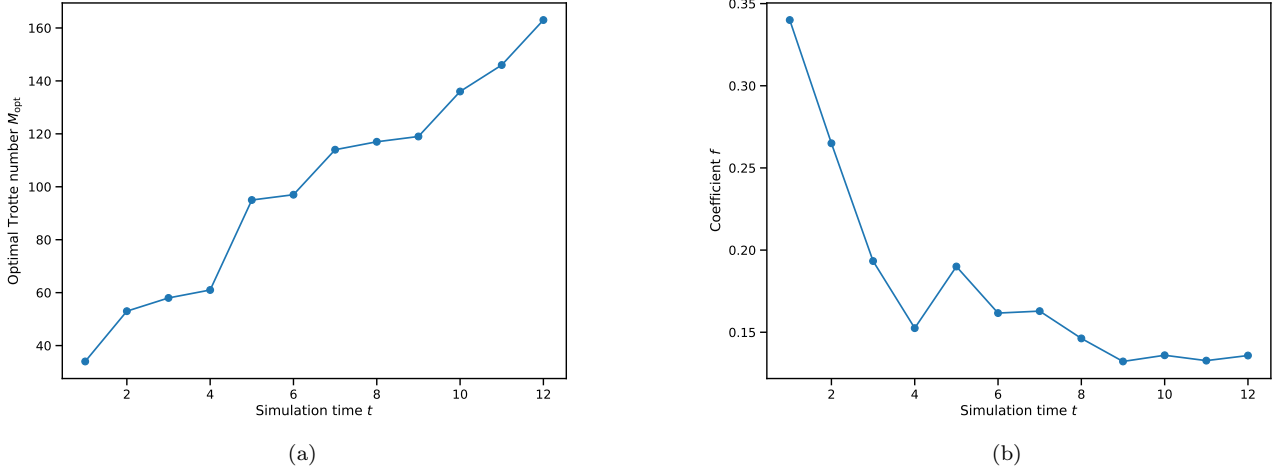


FIG. 7. Scaling of (a) the optimal Trotter number M_{opt} and (b) its coefficient f as a function of the simulation time t . In our numerical calculation, we set $n = 6$, $p_1 = 1 \times 10^{-5}$, $p_2 = 1 \times 10^{-4}$, $J = -1$, $B = 1$, and $t = 1, 2, \dots, 12$.

Appendix D: Validation of Eq. (7) by numerical simulation

Here, we analyze the scaling of the coefficient of the optimal Trotter number M_{opt} as a function of the simulation time t to validate Eq. (7). In Fig. 7a, we show that the scaling of the optimal Trotter step M_{opt} for the dynamics of 1D TFI as a function of the simulation time t , where M_{opt} is obtained numerically. It is observed that the optimal Trotter step increases as the simulation time increases, as expected. Then, we also calculate the scaling of the coefficient of the optimal Trotter number f as a function of the simulation time t , where f can be given by

$$f = \frac{M_{\text{opt}}}{|t| \sqrt{\frac{|J||B|}{p_2}}}.$$

From Fig. 7b, we confirm that f decreases until $t = 8$, but remains constant thereafter. Thus, our derived scaling of the optimal Trotter number shown in Eq. (7) can be valid when the simulation time is sufficiently long.

As discussed above, the coefficient for the optimal Trotter number can be obtained by combining theoretical analysis with numerical calculations. We also expect that regression analysis would be needed when we execute quantum simulations that are intractable for classical computers using actual quantum computers.

Appendix E: Shot noise on observable estimation by Trotter subspace expansion

In the previous section, we have explained that the quantum circuits in Figs. 2 and 3 with an infinite number of measurements give the expectation values for the ansatz states. In practice, expectation values of observables differ from the ideal ones because the total number of measurements is finite, which is called the shot noise. The expectation value of an observable A with finite measurements could be expressed as $\langle A \rangle_{\text{est}} + \delta A_{\text{est}}$, where δA_{est} stands for the deviation due to the shot noise. In our numerical simulation, we consider δA_{est} by adding the Gaussian noise whose amplitude is determined by $\text{Var}[A_{\text{est}}]$ to the expectation value without shot-noise. $\text{Var}[A_{\text{est}}]$ is composed of each variance of the Pauli observables shown in Fig. 2. More precisely, in our numerical simulations, we consider the shot noise according to the following procedure:

1. Compute an expectation value of all of the Pauli observables shown in Fig. 2 or Fig. 3 without shot noise.
2. Compute the corresponding single-shot variances: $\text{Var}[(X \otimes I^{\otimes 2})_{P_\alpha}]$, $\text{Var}[(Y \otimes I^{\otimes 2})_{P_\alpha}]$, and $\text{Var}[(X \otimes I^{\otimes 2})_I]$.
3. Generate the Gaussian noise $\mathcal{N}(0, V_{\text{single}}/N_{\text{circ}})$, where V_{single} and N_{circ} denote one of the single-shot variances in 2 and the number of measurements allocated for one quantum circuit to obtain one expectation value, respectively.

4. Add the Gaussian noise to the ideal expectation value.

5. Using the results from 4, output the estimator.

In the following, we will show the single-shot variance of the Pauli observables and then theoretically analyze the single-shot variance of the estimator with the Trotter subspace expansion.

1. Single-shot variance of Pauli observables

We discuss the single-shot variance of Pauli observables P_α or the identity I using the quantum circuits shown in Fig. 2: $\text{Var}\left[\left(X \otimes I^{\otimes 2}\right)_{P_\alpha}\right]$, $\text{Var}\left[\left(Y \otimes I^{\otimes 2}\right)_{P_\alpha}\right]$, and $\text{Var}\left[\left(X \otimes I^{\otimes 2}\right)_I\right]$. By definition, we obtain

$$\begin{aligned}\text{Var}\left[\left(X \otimes I^{\otimes 2}\right)_{P_\alpha}\right] &= \left\langle\left(X \otimes I^{\otimes 2}\right)_{P_\alpha}^2\right\rangle - \left\langle X \otimes I^{\otimes 2}\right\rangle_{P_\alpha}^2 \\ &= \left\langle I^{\otimes 3}\right\rangle_{P_\alpha} - \left\langle X \otimes I^{\otimes 2}\right\rangle_{P_\alpha}^2 \\ &= 1 - \left\langle X \otimes I^{\otimes 2}\right\rangle_{P_\alpha}^2.\end{aligned}\quad (\text{E1})$$

Also, the single-shot variance $\text{Var}\left[\left(X \otimes I^{\otimes 2}\right)_I\right]$ is given by

$$\begin{aligned}\text{Var}\left[\left(X \otimes I^{\otimes 2}\right)_I\right] &= \left\langle I^{\otimes 3}\right\rangle_I - \left\langle X \otimes I^{\otimes 2}\right\rangle_I^2 \\ &= 1 - \text{Tr}(\rho_i \rho_j)^2,\end{aligned}\quad (\text{E2})$$

where we use Eq. (C1).

2. Single-shot variance of the estimator with the Trotter subspace expansion

Here we give the theoretical analysis of the single-shot variance of the estimator with the Trotter subspace expansion. The expectation value for the ansatz state using the Trotter subspace is given by

$$\langle A \rangle_{\text{est}} = \frac{\sum_\alpha c_\alpha \left(\sum_{i=0}^{n'} g_i^2 \text{Tr}(\rho_i^2 P_\alpha) + 2 \sum_{i < j} g_i g_j \text{Tr}\left(\frac{\rho_i \rho_j + \rho_j \rho_i}{2} P_\alpha\right) \right)}{\sum_{i,j=0}^{n'} g_i g_j \text{Tr}(\rho_i \rho_j)}.$$

Using the quantum circuits shown in Fig. 2 and Eq. (C2), the above expression could be rewritten as

$$\langle A \rangle_{\text{est}} = \frac{\sum_\alpha c_\alpha \left(\sum_{i=0}^{n'} g_i^2 \left\langle X \otimes I^{\otimes 2} \right\rangle_{P_\alpha} + 2 \sum_{i < j} g_i g_j \left\langle X \otimes I^{\otimes 2} \right\rangle_{P_\alpha} \right)}{\sum_{i,j=0}^{n'} g_i g_j \left\langle X \otimes I^{\otimes 2} \right\rangle_I}. \quad (\text{E3})$$

Note that the first term of numerator $\left\langle X \otimes I^{\otimes 2} \right\rangle_{P_\alpha}$ depends on ρ_i , and the second term of numerator $\left\langle X \otimes I^{\otimes 2} \right\rangle_{P_\alpha}$ and the denominator $\left\langle X \otimes I^{\otimes 2} \right\rangle_I$ depend on ρ_i and ρ_j .

It is known that a variance of a ratio of two independent random variables F/G could be approximated as

$$\text{Var}\left[\frac{F}{G}\right] = \frac{1}{\langle G \rangle^2} \left[\text{Var}[F] + \left\langle \frac{F}{G} \right\rangle^2 \text{Var}[G] \right].$$

Using this approximation and Eq. (E3), we obtain the variance of the estimator:

$$\begin{aligned}\text{Var}[A_{\text{est}}] &= \frac{1}{\left(\sum_{i,j=0}^{n'} g_i g_j \left\langle X \otimes I^{\otimes 2} \right\rangle_I \right)^2} \\ &\times \left[\sum_\alpha \sum_{i,j=0}^{n'} c_\alpha^2 g_i^4 \text{Var}\left[\left(X \otimes I^{\otimes 2}\right)_{P_\alpha}\right] + 4 \sum_\alpha \sum_{i < j} c_\alpha^2 g_i^2 g_j^2 \text{Var}\left[\left(X \otimes I^{\otimes 2}\right)_{P_\alpha}\right] + \langle A \rangle_{\text{est}}^2 \sum_{i,j=0}^{n'} g_i^2 g_j^2 \text{Var}\left[\left(X \otimes I^{\otimes 2}\right)_I\right] \right].\end{aligned}\quad (\text{E4})$$

Substituting Eqs. (E1) and (E2) into Eq. (E4), we obtain

$$\begin{aligned} \text{Var}[A_{\text{est}}] &= \frac{1}{\left(\sum_{i,j=0}^{n'} g_i g_j \text{Tr}(\rho_i \rho_j)\right)^2} \\ &\times \left[\sum_{\alpha} \sum_{i,j=0}^{n'} c_{\alpha}^2 g_i^4 \left(1 - \text{Tr}(\rho_i^2 P_{\alpha})^2\right) + 4 \sum_{\alpha} \sum_{i < j} c_{\alpha}^2 g_i^2 g_j^2 \left\{ 1 - \text{Tr}\left(\frac{\rho_i \rho_j + \rho_j \rho_i}{2} P_{\alpha}\right)^2 \right\} + \langle A \rangle_{\text{est}}^2 \sum_{i,j=0}^{n'} g_i^2 g_j^2 \left(1 - \text{Tr}(\rho_i \rho_j)^2\right) \right]. \end{aligned}$$

Appendix F: Shot noise on observable estimation by virtual distillation

Here, we give the theoretical analysis of the single-shot variance of the estimator using virtual distillation (VD). Suppose that we would like to obtain the expectation value of an observable $A = \sum_{\alpha=1}^L c_{\alpha} P_{\alpha}$, where P_{α} is a Pauli operator. For simplicity, we use two copies of noisy states for VD. The error-mitigated expectation value with VD is given by

$$\begin{aligned} \langle A \rangle_{\text{est}} &= \frac{\text{Tr}(\rho^2 A)}{\text{Tr}(\rho^2)}, \\ &= \frac{\sum_{\alpha=1}^L c_{\alpha} \text{Tr}(\rho^2 P_{\alpha})}{\text{Tr}(\rho^2)}. \end{aligned}$$

Using the quantum circuits shown in Fig. 2 and Eqs. (C1) and (C2), where we set $\rho_i = \rho_j = \rho$, the above expression could be rewritten as

$$\langle A \rangle_{\text{est}} = \frac{\sum_{\alpha=1}^L c_{\alpha} \langle X \otimes I^{\otimes 2} \rangle_{P_{\alpha}}}{\langle X \otimes I^{\otimes 2} \rangle_I}.$$

Similar to Sec. E 2, the variance of the estimator can be approximated by

$$\begin{aligned} \text{Var}[A_{\text{est}}] &= \frac{1}{\langle X \otimes I^{\otimes 2} \rangle_I^2} \left[\sum_{\alpha=1}^L c_{\alpha}^2 \text{Var}[(X \otimes I^{\otimes 2})_{P_{\alpha}}] + \langle A \rangle_{\text{est}}^2 \text{Var}[(X \otimes I^{\otimes 2})_I] \right] \\ &= \frac{1}{\text{Tr}(\rho^2)^2} \left[\sum_{\alpha=1}^L c_{\alpha}^2 \left(1 - \text{Tr}(\rho^2 P_{\alpha})^2\right) + \langle A \rangle_{\text{est}}^2 \left(1 - \text{Tr}(\rho^2)^2\right) \right]. \end{aligned}$$